UCRL-50419

UCRL-50419

COMPUTER CALCULATIONS OF THE GASBUGGY EVENT

J. T. Cherry
D. B. Larson
E. G. Rapp

May 10, 1968

UNIVERSITY of CALIFORNIA
LIVERMORE

TID-4500, UC-35
Nuclear Explosions—
Peaceful Applications

Lawrence Radiation Laboratory
UNIVERSITY OF CALIFORNIA
LIVERMORE

UCRL-50419

COMPUTER CALCULATIONS OF THE GASBUGGY EVENT

J. T. Cherry
D. B. Larson
E. G. Rapp

May 10, 1968

COMPUTER CALCULATIONS OF THE GASBUGGY EVENT

Abstract

Shock-wave effects calculations of the Gasbuggy gas stimulation experiment have been made using a one-dimensional Lagrangian code, SOC. The detailed material description used for the equation of state of the rocks is presented along with the results of the calculations. Preliminary data from reentry of the emplacement hole indicate that the chimney height and available time of arrival data agree with predictions.

Introduction

The purpose of this paper is to describe the equation of state used and results of calculation of shock-wave effects for the Gasbuggy gas stimulation experiment. This effort was motivated by the philosophy that the successful industrial application of nuclear explosions in the years ahead will evolve as the result of a systematic scientific approach to understanding each experiment. Such a philosophy was employed in the Gasbuggy Event as a precedent for future experiments.

The application of modern computational techniques to underground nuclear engineering is an exciting, yet extremely challenging new field of research. Both experimental and theoretical methods are employed in this type of analysis. The successful application of these techniques has opened new fields of scientifically directed applications, such as the use of nuclear explosions in mining, excavation, and the formation of underground storage cavities.

The growing experience in this field of research indicates that a careful, representative description of the medium followed by calculations (using appropriate hydrodynamic calculational models) presents a much improved description of shock effects when compared with the often used scaling techniques.[1]

CALCULATIONAL PROCEDURES

The models currently employed for shock-wave effects calculations are SOC, a one-dimensional Lagrangian code and TENSOR, a two-dimensional Lagrangian code.[2,3] These codes combine the equation of motion of a material under stress with a unique description of that material's

behavior. Figure 1 illustrates the calculational process for establishing a propagating stress field. The equation of motion is obtained by combining the conservation of mass, linear momentum, and angular momentum equations of continuum mechanics. This equation, in differenced form, provides a functional relation between stress gradients and accelerations. References 2, 3 and 4 discuss the differencing methods for both the equation of motion and the strain tensor.

In this calculational process, at time t, the stress is known in each mass element in the medium. The stress

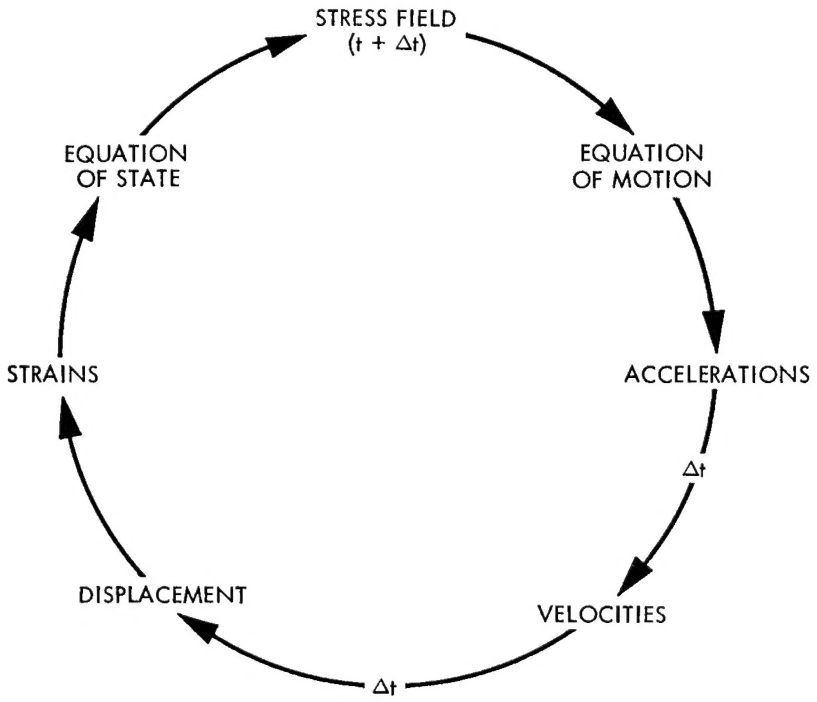

Fig. 1. Feed back loop for stress wave.

gradient across each element produces an acceleration. These accelerations produce new velocities which in turn displace (strain) each point in the medium, and cause new stresses. Time is incremented by the amount used to produce displacement from acceleration. This loop is repeated until the response of the numerical model allows a prediction of the results of the experiment.

The scheme that relates strain to stress is called the equation of state of the medium. We derive this description of the material behavior by field and laboratory experiments on representative samples of the shot media. Inherent in the equation of state is the ability to describe elastic, fractured, plastic, liquid and gaseous modes of behavior, and also to allow acceptable transitions from one mode to another.

In order to obtain a meaningful pre-shot calculation of the stress induced effects of a nuclear explosion on the

surrounding rock media, a number of logging tests and laboratory tests on selected core samples must be performed.

The logging tests pertinent to the equation of state development are:

(1) Density log.
(2) Elastic velocity log.
    (a) Compressional velocity.
    (b) Shear velocity.

Hopefully, these logs will permit a judgment of both the layering of the medium and the choice of core for laboratory testing.

The core tests required are:

(1) Hydrostatic compressibility up to 40 kbar.
(2) Strength tests.
    (a) Triaxial tests.
    (b) Tension tests.
(3) Hugoniot elastic limit.
(4) High-pressure Hugoniot data and chemistry for those rocks near the point of detonation.

When properly interpreted, these tests give the strength, compressibility, and rigidity modulus of a material. The source description is obtained by calculating the volume of rock that will be shocked-vaporized by a particular yield. The explosive yield is then distributed uniformly within the vaporized region and the stress field is allowed to propagate from this source. Reference 5 gives the gas equation of state and the vaporized radius for a number of rock materials.

THE CHIMNEY MODEL

Strength properties of granite and dolomite have been used to calculate the extent of cracking from the Hardhat (5 kt, 290 m deep, granite) and Handcar (12 kt, 402 m deep, dolomite) Events.

Figure 2 gives the strength curves for the two materials. Figure 3 shows the hydrostatic compressibility and Poisson's ratio for each material.

As mentioned above, the strength, compressibility and Hugoniot data and Poisson's ratio (along with the source description) form the basic input for the SOC stress wave code. The results of the SOC calculation on Hardhat and Handcar are shown in Fig. 4. It is interesting that the calculated extent of cracking for both Hardhat and Handcar agrees with the observed chimney height to within 14%. The calculated and measured cavity radii are in excellent agreement for both experiments. If strength of material and shock-induced cracking control the chimney formation, then it is no longer surprising that a 12 kt source in dolomite produces a smaller chimney than a 5 kt source in granite.

From these observations it is proposed that chimney formation should extend above the cavity a distance equal to or greater than the shock-induced cracking radius predicted by the SOC code. An exception to this model would occur whenever material properties were such that the cavity bulked full before this radius was reached.

GASBUGGY EQUATION OF STATE

The important formations and interface positions are illustrated in Fig. 5 for the Gasbuggy experiment. The experiment was so designed that a complete equation of state description was necessary

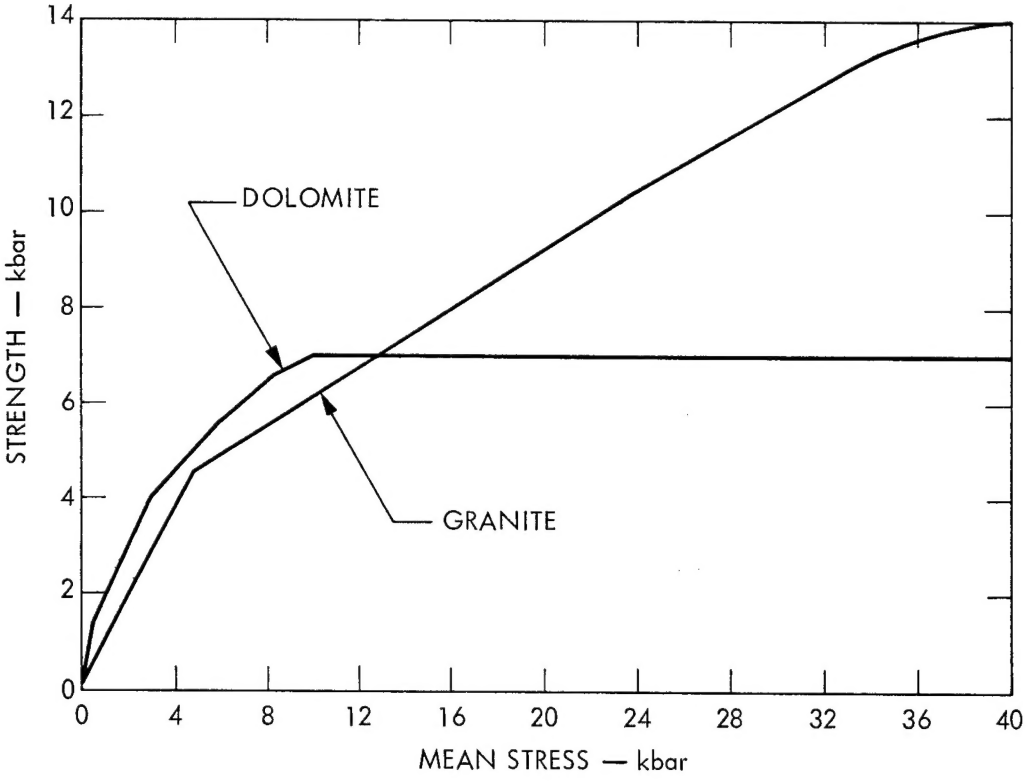

Fig. 2. Strength of dolomite and granite.

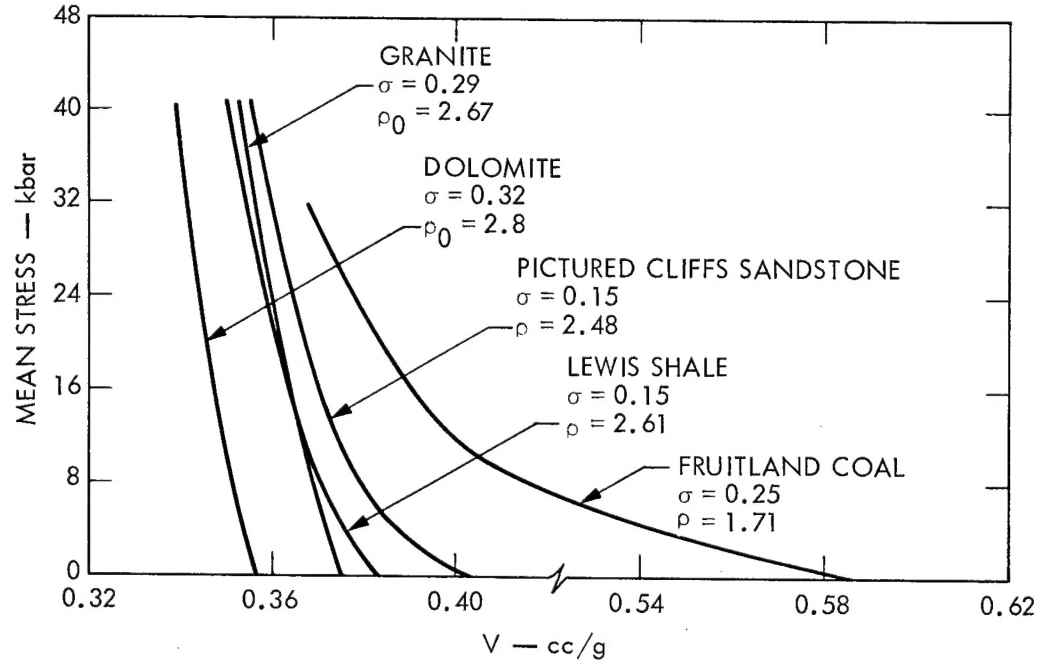

Fig. 3. Hydrostatic compressibility of dolomite, granite, sandstone, shale, and coal.

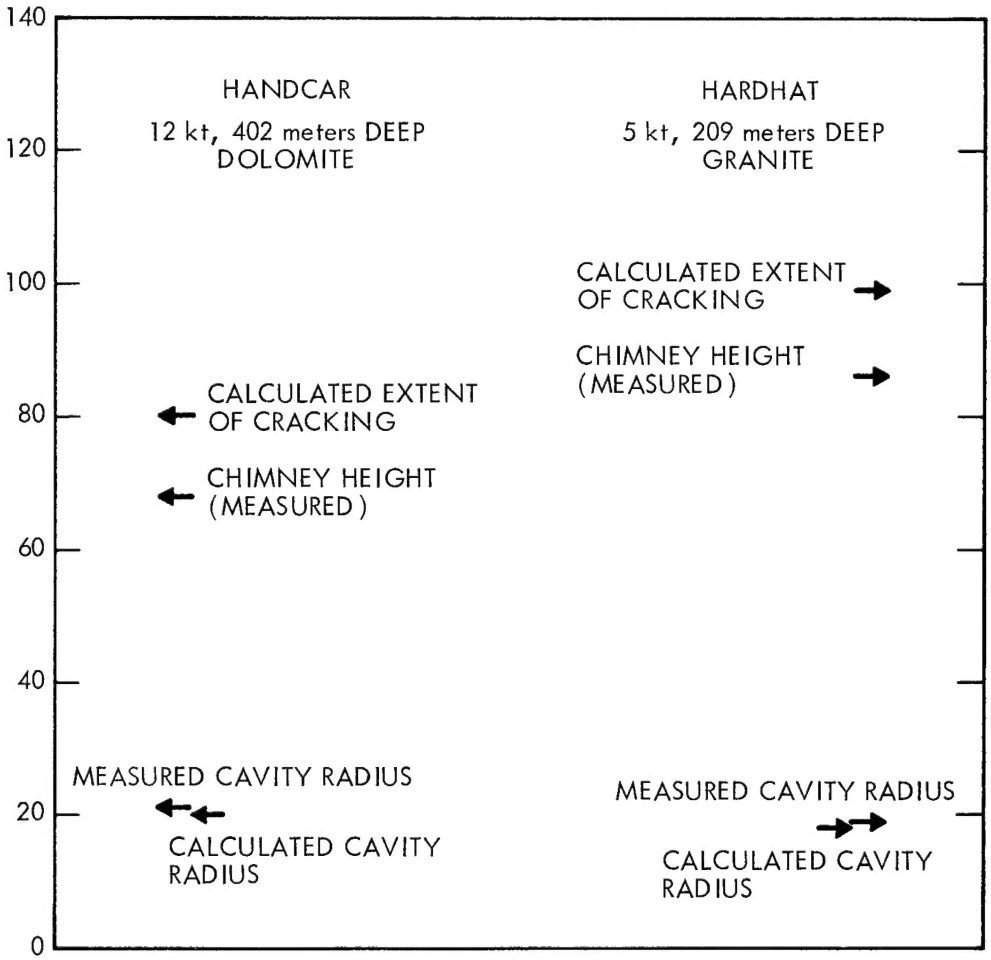

Fig. 4. Calculations for Handcar and Hardhat.

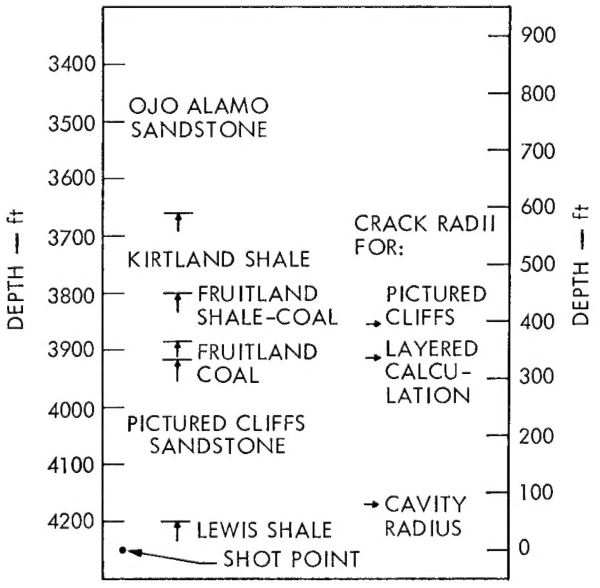

Fig. 5. Results of preliminary Gasbuggy calculations.

for the Lewis shale formation. The equation of state of the Pictured Cliffs sandstone was obtained to stress levels of 200 kbar. Only limited compression and strength data was required for the other formations since they were exposed to stress levels of less than a few kilobars.

Figure 6 shows the Hugoniot data that were obtained from the Lewis shale and the Pictured Cliffs sandstone. Figure 7 compares this data with hydrostatic compression data taken by D. Stephens. The offset between these two sets of data appears (in both materials) to be consistent with the triaxial strength data

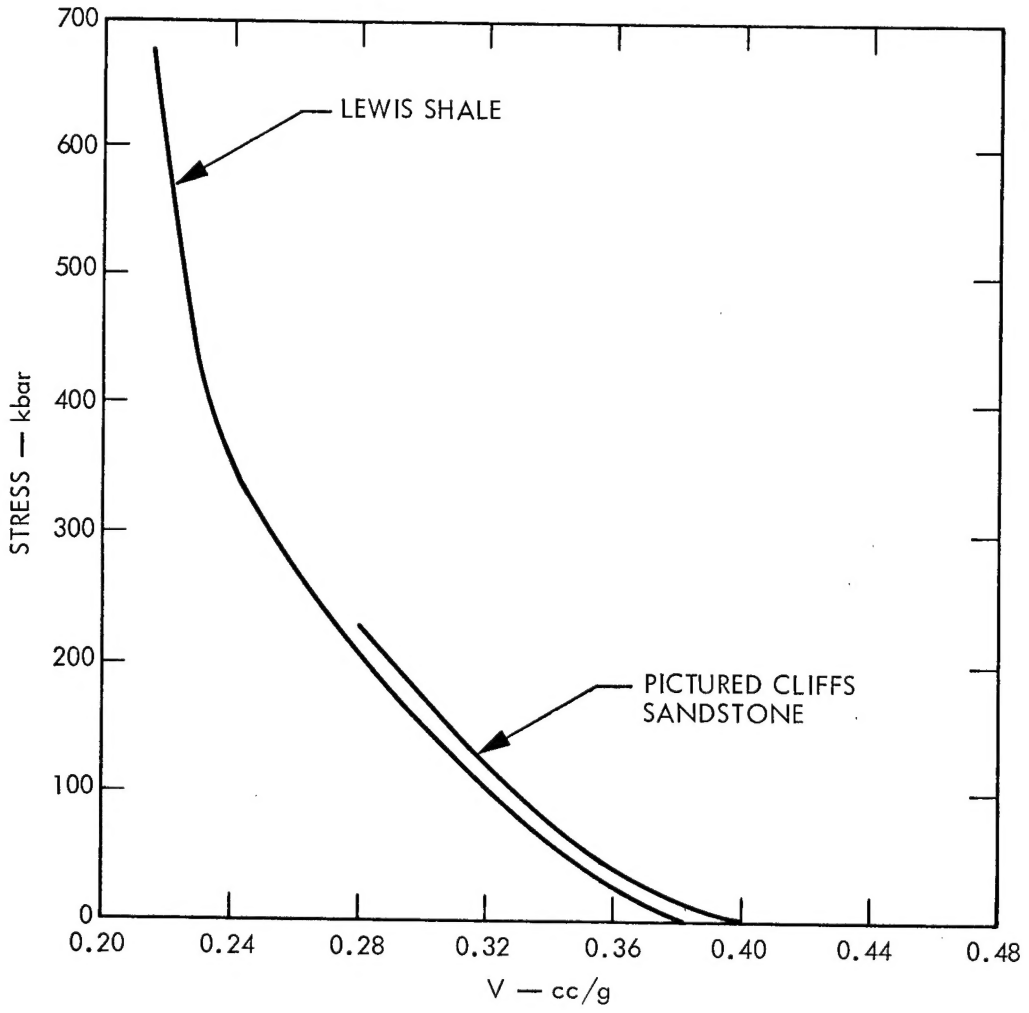

Fig. 6. Hugoniot data for Lewis shale and Pictured Cliffs sandstone.

shown in Fig. 8. The effective strength as measured in the comparison was derived from the expression

$$\sigma_x = \sigma_m + 4/3\ K$$

where σ_x is the uniaxial stress, σ_m is the mean stress, and K is the strength at a given mean stress. The agreement at the two different strain rates indicates that the assumption of negligible strain-rate effects in the use of statically determined equation of state data is justified.

The equation of state description for the Gasbuggy materials is given in Table I. These data have been chosen as a unique and representative description of the media involved based upon the tests mentioned in the introduction. Implied in this description is an averaging process inherent in the logs and a bias towards the more competent material used in the laboratory testing.

CALCULATIONS

The input equation of state description presented in Table I was used in two

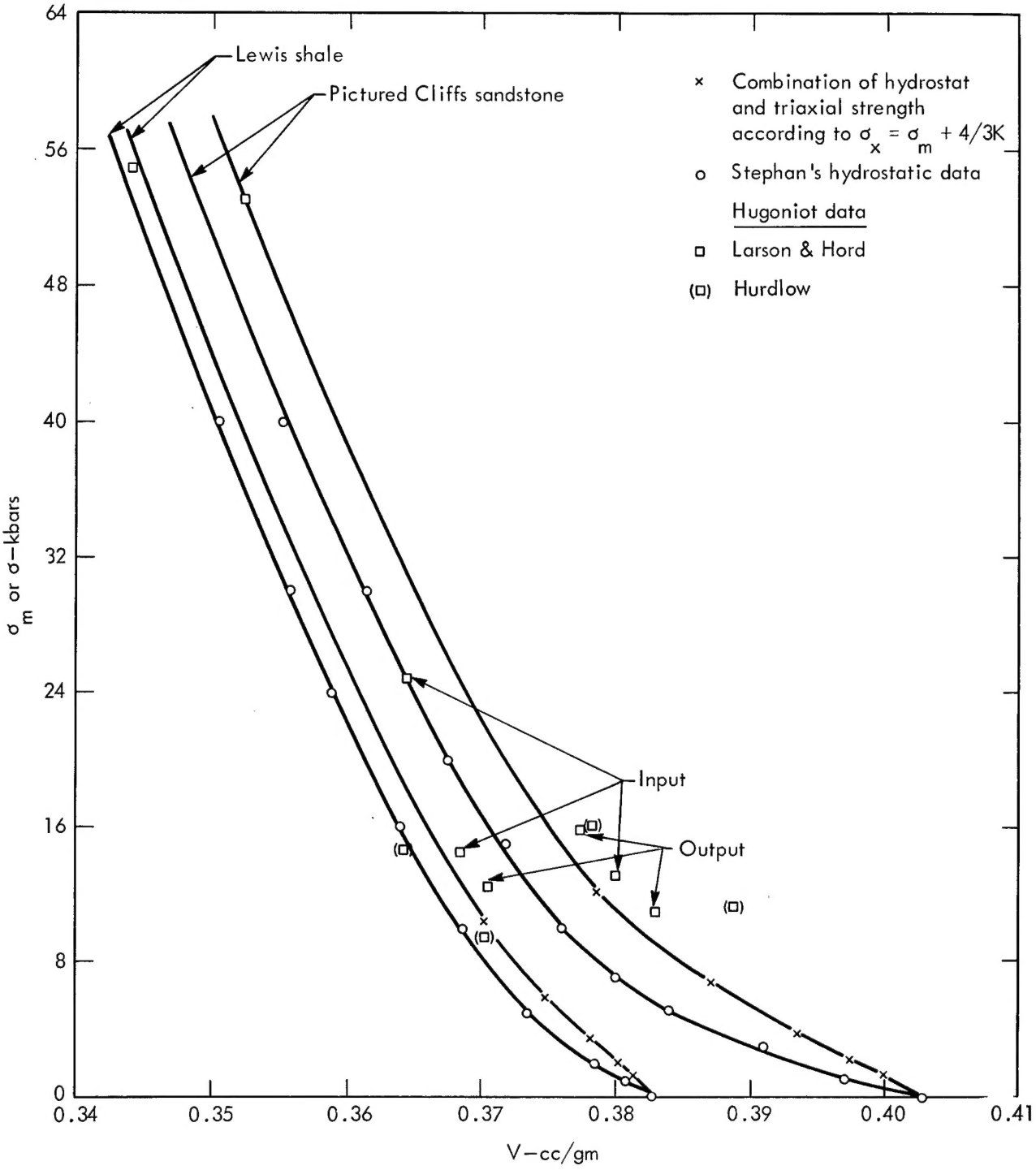

Fig. 7. The hydrostats and calculated Hugoniot.

one-dimensional calculations assuming 25 kt of energy deposited at 4250 ft. The first calculation ignored all interfaces above the Pictured Cliffs formation and predicted a cavity radius of 78 ft and a crack radius extending to 393 ft. When the other layers were included in the calculations, the Fruitland coal layer

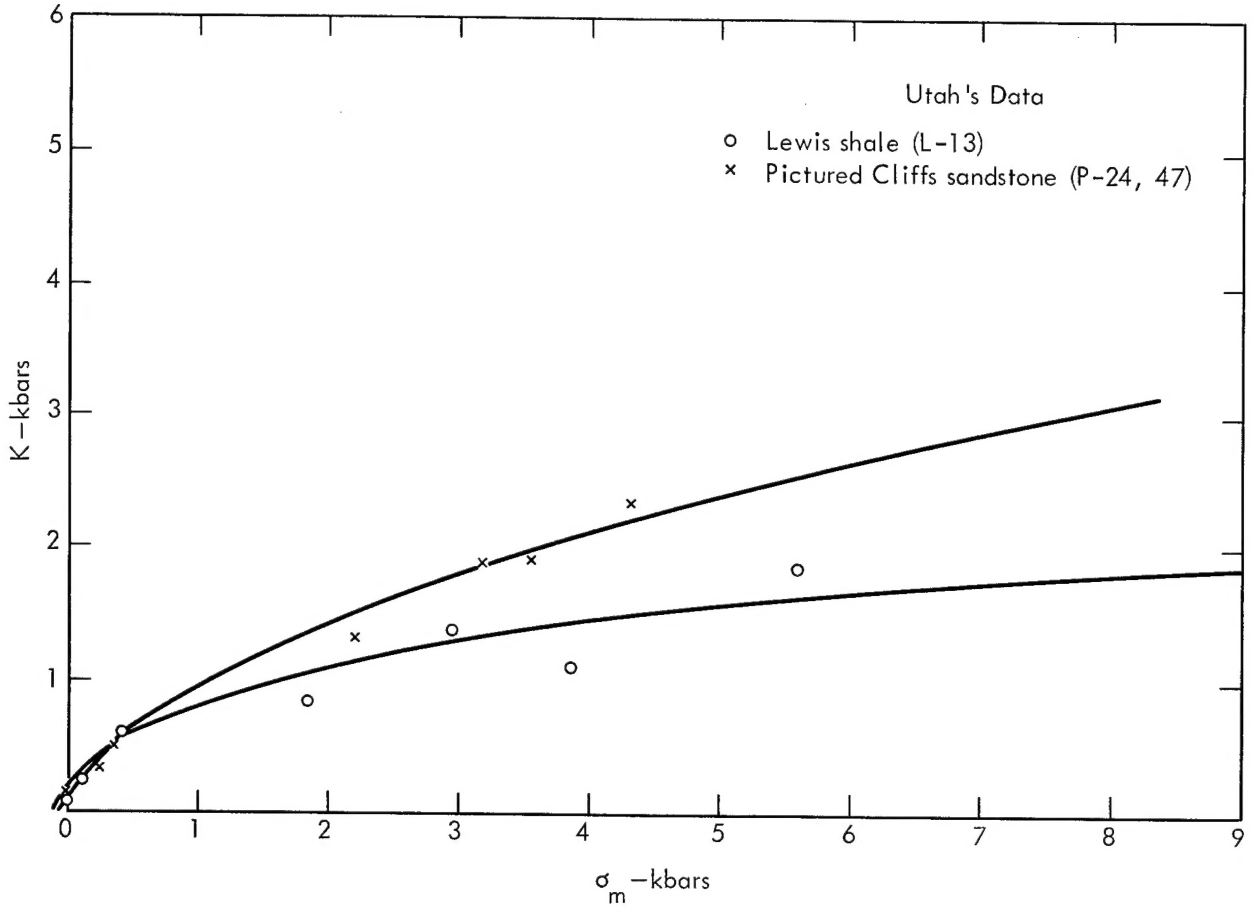

Fig. 8. Triaxial strength data for Lewis shale and Pictured Cliffs sandstone.

Table I. This table includes the parameters that are used in conjunction with compression and strength data to generate equation of state descriptions for the Gasbuggy calculations. The heats of fusion and vaporization that are given are for SiO_2.

Material type	Region thickness (ft)	Density (g/cc)	Comp. velocity log (ft/sec)	Total water content (% by wt)	Compressibility (megabars)	Poisson's ratio	Heat of vapor 10^{12}erg/cc	Heat of fusion 10^{12}erg/cc
Lewis shale	Shot point to 4202	2.61	13,700	3.5	0.191	0.15	4.759×10^{-1}	1.259×10^{-1}
Pictured Cliffs sandstone	4202 to 3915	2.48	13,520	4.5	0.134	0.15		
Fruitland coal	3915 to 3882	1.71	8,850		0.0602	0.25		
Fruitland shale	3882 to 3800	2.49	11,700		0.132	0.15		
Kirtland shale	3800 to 3650	2.58	14,070		0.240	0.15		

influenced the results enough to stop the cracking at that boundary 334 ft from the detonation point. The 393 ft cracking radius (determined in the first calculation) is a measure of the expected lateral cracking within the Pictured Cliff formation.

Figures 9, 10, 11, and 12 are calculated radial stress profiles at 10, 20, 45, and 75 m from the detonation point. Figures 11 and 12 clearly show the elastic precursor propagating ahead of the driving stress-wave. The precursor stress level is a measure of the

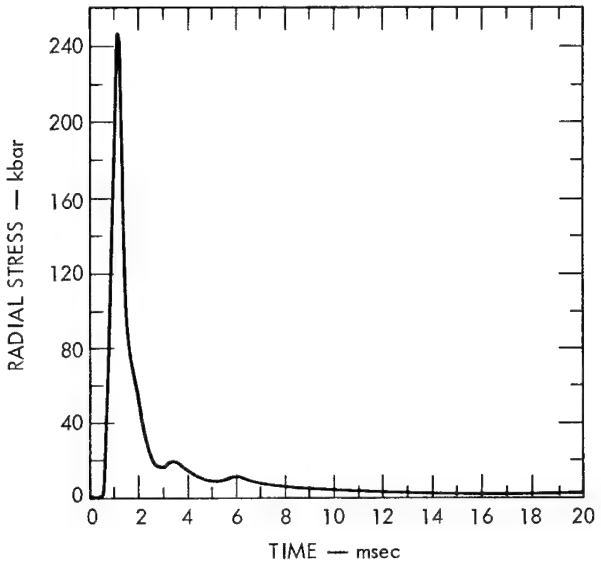

Fig. 9. Radial stress vs time for the radius at 10 meters.

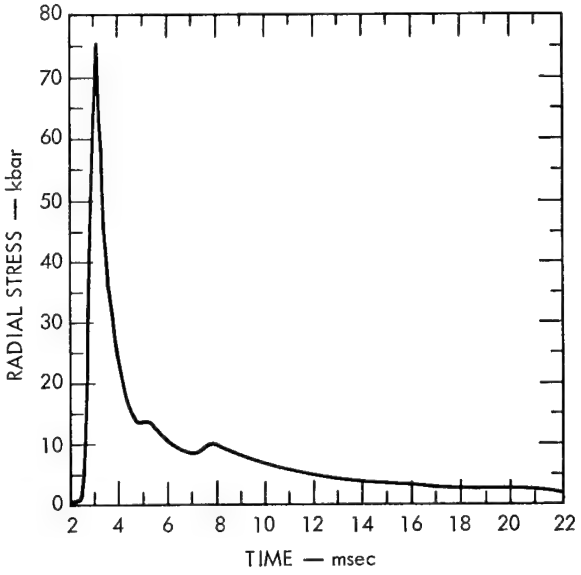

Fig. 10. Radial stress vs time for the radius at 20 meters.

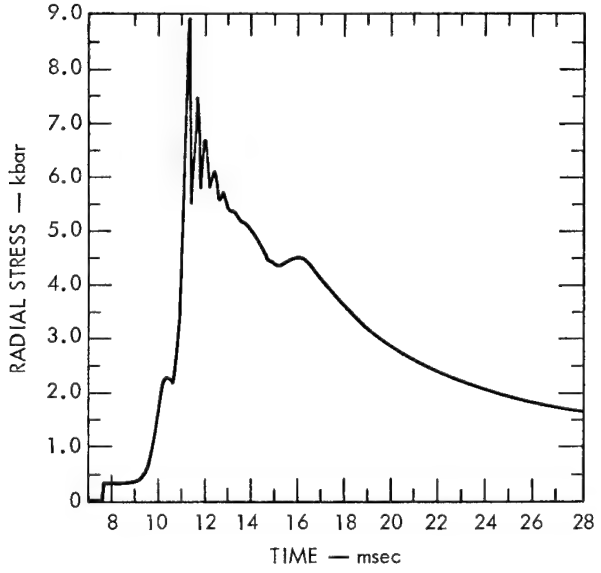

Fig. 11. Radial stress vs time for the radius at 45 meters.

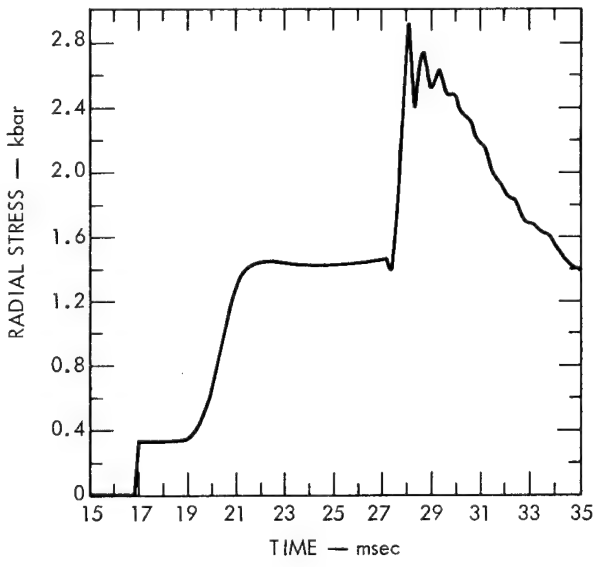

Fig. 12. Radial stress vs time for the radius at 75 meters.

threshold for dynamic failure of the material. Figure 9 shows behavior within the Lewis shale, while Figs. 10, 11, and 12 reveal behavior patterns within the Pictured Cliffs sandstone formation.

The calculations have indicated that, given a 25 kt source at 4250 ft, there will be material failure until the coal seam is reached at 3915 ft. This highly compressible but relatively strong material will stop the cracks from propagating above the Pictured Cliffs formation. As the cavity pressure subsides (and collapse takes place to fill the void) a competent coal layer should prevent collapse above this point. However, if this layer proves unstable, collapse could continue until a competent formation is reached (i. e., into the Fruitland shale formation).

The preliminary data that are now available from the actual experiment indicates that the energy source was close to the expected value of 25 kt (see Fig. 13). Reentry of the emplacement hole, the only postshot experiment in progress, has provided data which indicates that the coal layer was competent enough to halt collapse near the top of the Pictured Cliffs formation. This reentry drilling encountered a 6 ft void but no radioactivity at a depth of 3858 ft. However, at a depth of 3907 ft, a 9-ft void was encountered and radioactive xenon was detected at the surface indicating that the chimney had been located.

These preliminary results indicate that an accurate equation of state description of an experimental environment is

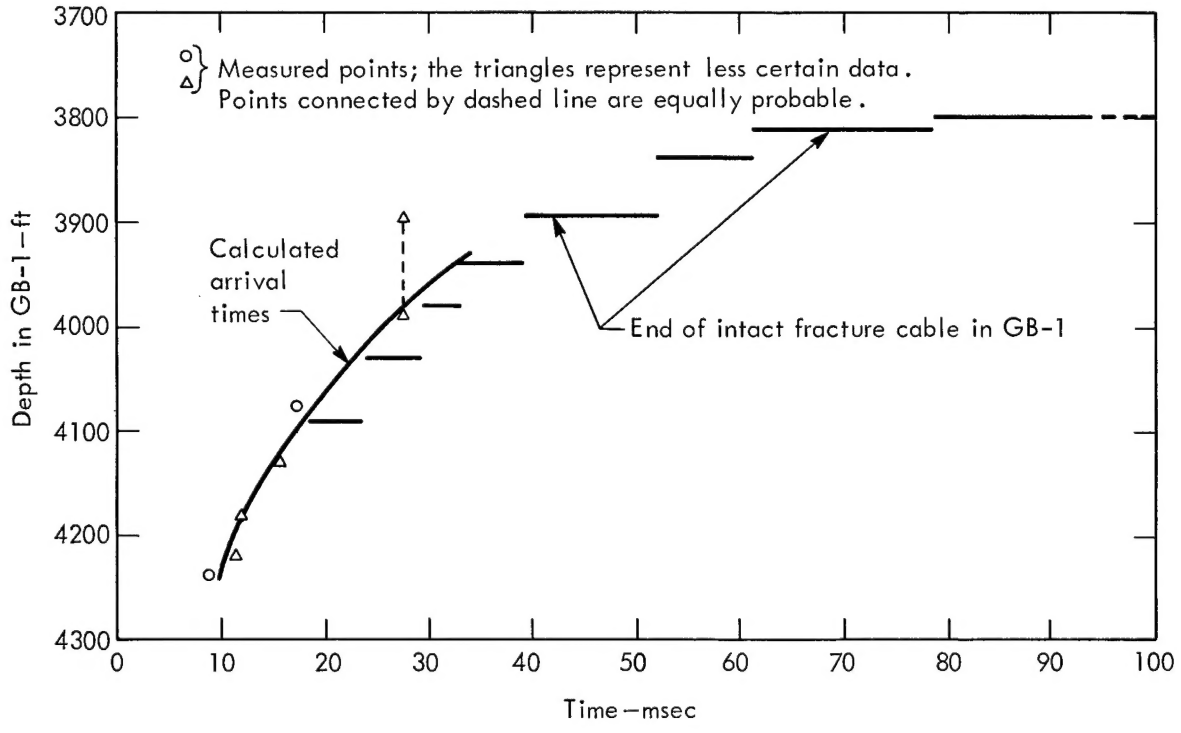

Fig. 13. Time of arrival of various radial distances.

basic to reliable predictive calculations. Furthermore, the success of incorporating a modern failure model into material behavior has dramatic implications when one considers the broad spectrum of earth material strengths that are encountered in dealing with underground nuclear applications.

References

1. Cherry, J. T., Larson, D. D., and Rapp, E. G., A Unique Description of the Failure of a Brittle Material, Lawrence Radiation Laboratory, Livermore, Rept. UCRL-70617 (1967).
2. Maenchen, G., and Sack, S., The Tensor Code, Lawrence Radiation Laboratory, Livermore, Rept. UCRL-7316 (1963).
3. Cherry, J. T., "Computer Code of Explosion Produced Craters," Intern. J. of Rock Mech., 4, 1-22 (1967).
4. Wilkins, M. L., Calculations of Elastic-Plastic Flow, Lawrence Radiation Laboratory, Livermore, Rept. UCRL-7322 (1963).
5. Butkovich, T. R., The Gas Equation of State of Natural Materials, Lawrence Radiation Laboratory, Livermore, Rept. UCRL-14729 (1966).

Distribution

LRL Internal Distribution

Michael M. May

T. R. Butkovich

J. T. Cherry

J. W. Hadley

H. C. Heard

J. R. Hearst

G. H. Higgins

F. Holzer

W. R. Hurdlow

J. S. Kahn

J. A. Korver

J. B. Knox

D. B. Larson 10

A. E. Lewis

D. B. Lombard

M. D. Nordyke

E. G. Rapp

D. E. Rawson

H. L. Reynolds

L. A. Rogers

C. J. Sisemore

D. R. Stephens

T. S. Sterrett

R. W. Terhune

H. A. Tewes

G. C. Werth

LRL Internal Distribution (Continued)

E. White

W. R. Woodruff

TID Berkeley

TID File 30

External Distribution

W. J. Murri
C. Peterson
R. Linde
Stanford Research Institute
Menlo Park, California

TID-4500 Distribution, UC-35, Nuclear Explosions—Peaceful Applications 292

Printed in USA. Available from the Clearinghouse for Federal Scientific and Technical Information, National Bureau of Standards, U. S. Department of Commerce, Springfield, Virginia 22151
Price: Printed Copy $3.00; Microfiche $0.65.

KP/lh